JOURNAL OF MATERIALS SCIENCE 30 (1995) 35–39

Acoustic investigation of porous silicon layers

R. J. M. DA FONSECA, J. M. SAUREL, A. FOUCARAN*, J. CAMASSEL*, E. MASSONE*, T. TALIERCIO*
*Laboratoire de Microacoustique de Montpellier, cc079, and *Groupe d'Etude des Semiconducteurs (U.R.A. 0357), cc074, Université des Sciences et Techniques du Languedoc, Place E. Bataillon, 34095 Montpellier cedex 5, France*
Y. BOUMAIZA
Laboratoire de Semiconducteurs, Institut de Physique BP12, Université de Annaba, Algeria

Porous silicon (PS) layers are formed on p^+-type silicon wafers by electrochemical anodization in hydrofluoric acid solutions. Microechography and acoustic signature, $V(z)$, have been performed at 1.5 GHz and 600 MHz, respectively, in order to study the elastic properties of PS layers. The thicknesses of PS layers were measured and longitudinal, shear and Rayleigh velocities and Young's modulus were obtained as a function of porosity. Equations showing the porosity dependence of bulk wave velocities and Young's modulus have also been proposed.

1. Introduction

Porous silicon (PS) is electrochemically formed by anodic dissolution of silicon in a hydrofluoric acid solution. It has been extensively studied since it was discovered by Turner [1] in 1958 and, particularly, from the recent observations where porous silicon exhibited strong visible luminescence at room temperature (suggesting promising applications in silicon-based optoelectronic devices [2]). Other fields of application exist for PS: one in full insulation by porous oxidized silicon [3] or the FIPOS technique, and others in silicon micromachining and microsensors. In fact, depending on the electrolysis conditions [4], this material presents a porous texture with pore diameters varying from 2–15 nm and a density varying from 20%–80% of that of the original substrate. This makes PS a very versatile material.

Despite these varied interests, the mechanical properties of PS layers have not been much studied. It is a well-established fact that many elastic parameters change drastically with increasing porosity. For instance, in aerogels the Young's modulus can be smaller by a factor of 10^4 than for non-porous silica glass [5]. Consequently, for many practical applications, it is important to characterize the mechanical behaviour of porous materials. However, for relatively thin specimens such as PS layers, conventional mechanical tests (strength, bending and compression loading) complicate the interpretation of elastic properties measurements and easily destroy the samples [6]. Otherwise, acoustic microscopy is a very good technique designed for this purpose, as far as small volumes are concerned. Furthermore, it is a non-destructive and easy to handle method which not only allows the determination of acoustic properties in microanalysis but also the detection of defects by acoustic imaging of both surfaces and subsurfaces of materials [7–10]. In this work, we show that the combination of acoustic techniques, more specifically the acoustic material signature, $V(z)$, and high-frequency microechography, allows one to determine routinely and independently the thickness, bulk wave velocity and Young's modulus of PS layers. Equations showing the porosity dependence of the longitudinal wave velocity and elastic modulus have also been derived.

2. Experimental procedure

2.1. Preparation of the PS layers

All PS layers were produced by anodization of silicon wafers in hydrofluoric acid solutions using platinum as a counter electrode. The silicon wafers used in the present experiments were p^+-type single crystals of (1 0 0) orientation with polished surfaces and about 15 mm × 15 mm × 0.30 mm in size. Hydrofluoric acid solutions concentration and current of anodization were controlled in order to obtain PS layers with different values of porosity and thickness. The porosity of PS layers was 20%–50% and it was calculated from the weight and volume of the specimens, taking the density of non-porous silicon as 2330 $kg\,m^{-3}$.

2.2. High-frequency microechography

To measure thickness and longitudinal wave velocity of the PS layers, high-frequency microechography was performed using a network analyser (HP 8753A) together with the S-parameter test set (HP 85046A). This equipment can measure reflection and transmission parameters as a function of frequency. Moreover, it is equipped with a Fourier transform processor which allows us to calculate equivalent response in the time domain (pulse response), with excellent time resolution ($\simeq 10^{-12}$ s). All the experiments were carried out

0022–2461 © 1995 Chapman & Hall

in reflection mode, i.e. measuring the S_{11}-parameter, defined as the ratio of the reflected to incident wave. Consequently, only a single ultrasonic transducer was used for transmitting and receiving the acoustic signal. The transducer was operated at a central frequency of 1.5 GHz and it was directly connected to the input of the S-parameter test set. Because high-frequency acoustic waves cannot propagate in air, we employed water to couple the transducer to the specimen. The non-porous face of a silicon wafer was put towards the transducer in order to avoid water penetration in the porous silicon layer. A schematic illustration is shown in Fig. 1. In this experimental configuration three echoes are detected by the transducer (see Fig. 2): the first echo from the H_2O–non-porous silicon interface at time t_0, the second one from the non-porous Si–PS layer interface at time t_1 and, finally, the third one from the PS layer–air interface at time t_2. Thickness and longitudinal wave velocity of PS layers were determined from the time delay, Δt, between these consecutive echoes and by using the following relations [9]

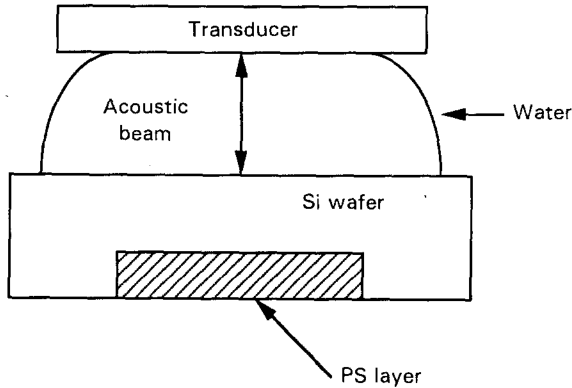

Figure 1 Schematic illustration of a porous silicon sample in high-frequency microechography measurements.

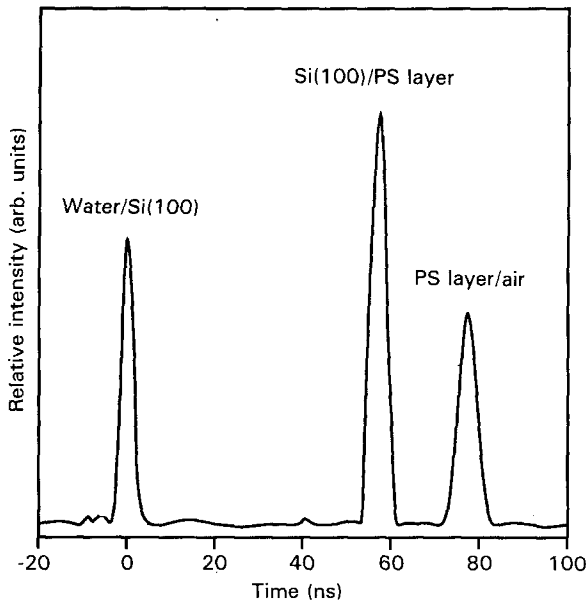

Figure 2 Microechographic spectrum of a PS sample. The echoes are due to the H_2O–Si wafer, Si wafer–PS layer and PS layer–air interfaces.

$$d = d_0 - \frac{V_{L0}}{2}(t_1 - t_0) \quad (1)$$

and

$$V_L = \frac{2d}{(t_2 - t_1)} \quad (2)$$

where d_0 is the total thickness of the silicon wafer, d is the thickness of the PS layer and V_{L0} and V_L are the longitudinal wave velocities for non-porous silicon and the PS layer, respectively. The time delay, Δt, between the echoes was measured to within 0.1% and V_{L0} was taken as 8435 m s^{-1} [11].

2.3. Acoustic signature, $V(z)$

In this study the acoustic microscope was used to measure more directly the Young's modulus of PS layers via the so-called acoustic material signature, also known as $V(z)$. This signature is obtained by recording the reflected acoustic signal variation, V, as a function of the sample defocus, z, when the latter is moved along the axis from the focal plane toward the transducer. As z varies, the $V(z)$ curves exhibit pseudo-oscillations due to the constructive and destructive interference between a narrow bundle of axial specular reflected waves and leaky surface waves. This interference phenomenon constitutes the acoustic material signature. For elastic characterization, the most significant and interesting mode in the $V(z)$ curves is the Rayleigh mode. In our $V(z)$ experiments, performed at an operating frequency of 600 MHz, the Rayleigh wave velocity, V_R, for each PS layer was precisely calculated from fast Fourier transform (FFT) spectra of $V(z)$ curves [10, 12].

As soon as the longitudinal and Rayleigh wave velocities were measured by the two acoustic methods described above, we could easily determine the shear wave velocity, V_S, by using the Viktorov's relation [13]

$$V_R = V_S \frac{0.718 - (V_S/V_L)^2}{0.750 - (V_S/V_L)^2} \quad (3)$$

Hence the Young's modulus, E, was related to the velocities V_L and V_S via the following expression

$$E = A \rho V_L^2 \quad (4)$$

where ρ is the density of the material and A is a quantity that depends on the ratio of shear wave velocity to the longitudinal wave velocity. Actually this parameter can be written as [13, 14]

$$A = \left(\frac{V_S}{V_L}\right)^2 \left[3 - 4\left(\frac{V_S}{V_L}\right)^2\right] \bigg/ \left[1 - \left(\frac{V_S}{V_L}\right)^2\right] \quad (5)$$

It should be noted that in Equations 3–5 the values of ρ, V_L and V_S change as a function of porosity. The data on velocities and mechanical properties of PS layers reported in the paper are based on the average of 20 tests.

3. Results and discussion

Rayleigh and shear velocities and the thickness for PS layers are summarized in Table I. For each specimen, the thickness measured by the ultrasonic method represents an average which was taken in 20 different zones of the material. These average values can be compared with the one obtained by micrometric measurement of the silicon substrate thickness after removing the PS layer. There was a reasonably good correspondence between the values obtained by the two methods, the maximum difference being less than 2%.

Fig. 3 shows some $V(z)$ curves for different values of porosity. It can be observed that the period of the pseudo-oscillations in $V(z)$ response decreases with the increase of porosity. This qualitative analysis is confirmed by the reduction of the Rayleigh velocity when calculated from FFT spectra of $V(z)$ curves. This last result indicates a decrease of the efficiency of stress-wave energy propagation as well as stiffness constants of the material with an increase of flaw density. These phenomena have also been found in other porous materials, as seen in relevant publications [15–17].

The experimental results of longitudinal wave velocity of PS layers as a function of porosity are shown in Fig. 4. In this figure, we also included the value of longitudinal velocity for non-porous silicon which was measured from a non-anodized silicon wafer. The distribution of the points suggests a linear behaviour between the longitudinal velocity, V_L, and the porosity, P, and shows that these parameters can be correlated by the equation

$$V_L = V_{L0}(1 - P)^k \quad (6)$$

where V_{L0} is the longitudinal velocity at zero porosity and k is an empirical constant. The values of V_{L0} and k were evaluated by a numerical analysis software and found to be 8570 m s^{-1} and 1.095, respectively.

Likewise we can express the porosity dependence of the shear-wave velocity by a similar expression to Equation 6, i.e.

$$V_S = V_{S0}(1 - P)^m \quad (7)$$

where V_{S0} is the shear velocity for non-porous silicon and m has a like definition to k in Equation 3. Because $\rho = \rho_0(1 - P)$ for air-saturated porous materials

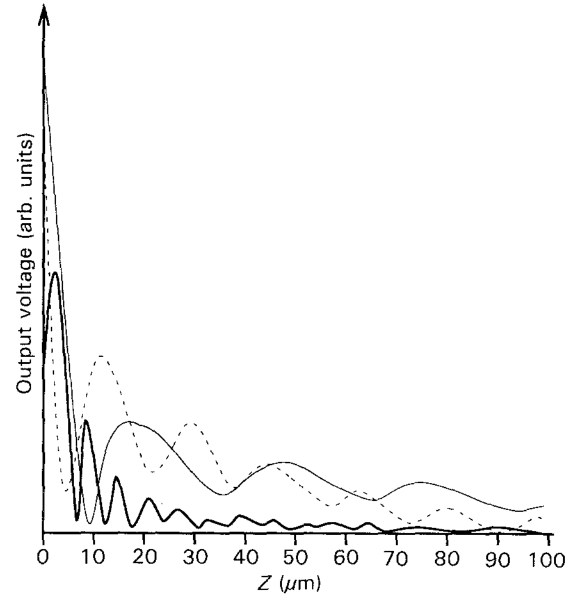

Figure 3 $V(z)$ curves of three different samples: (——) non-porous silicon, (- - -) PS layer-20% and (——) PS layer-47%.

[18, 19] where ρ_0 is the density at zero porosity, the Young's modulus, E, can be related directly to porosity by substituting Equations 6 and 7 into 4 and 5, then

$$E = B_0X^2(1 - P)^{q+s}\left[\frac{3 - 4X^2(1 - P)^q}{1 - X^2(1 - P)^q}\right] \quad (8)$$

where

$$B_0 = \rho_0 V_{L0}^2 \quad (9)$$

$$X = \frac{V_{S0}}{V_{L0}} \quad (10)$$

$$q = 2(m - k) \quad (11)$$

$$s = 2k + 1 \quad (12)$$

In order to fit the experimental results of Young's modulus, the constants B_0, X, q and s were evaluated numerically using ASYST subroutines [20] and they were found to be 165.30 GPa, 0.69, 0.18 and 3.22, respectively. The data agree reasonably with Equation 8, having correlation coefficient of 0.993. For Si (1 0 0) the theoretical value of A in Equation 4 is approximately equal to 1 (see the values of longitudinal and

TABLE I Thickness and velocities determined from the acoustic techniques for PS layers

Sample	Density, ρ (kg m^{-3})	Rayleigh velocity, V_R (m s^{-1})	Shear velocity[a], V_S (m s^{-1})	Layer thickness[b], d (μm)	Layer thickness[c], d (μm)
Non-porous Si	2330	5140 ± 30	5840 ± 50	290 ± 2	289 ± 2
PS-20%	1864	4005 ± 20	4450 ± 40	44 ± 0.5	45 ± 1
PS-28%	1678	3820 ± 20	4170 ± 40	65 ± 0.7	65 ± 1
PS-32%	1584	3320 ± 15	3645 ± 30	35 ± 0.4	35 ± 1
PS-35%	1515	2845 ± 15	3170 ± 30	52 ± 0.5	53 ± 1
PS-38%	1445	2695 ± 15	2970 ± 30	61 ± 0.7	60 ± 1
PS-47%	1221	2270 ± 15	2520 ± 30	105 ± 1	103 ± 1

[a] Shear velocities calculated from the experimental results of Rayleigh and Longitudinal velocities by using Equation 3.
[b] Thicknesses measured by the ultrasonic method.
[c] Thicknesses measured by etching off the PS layer.

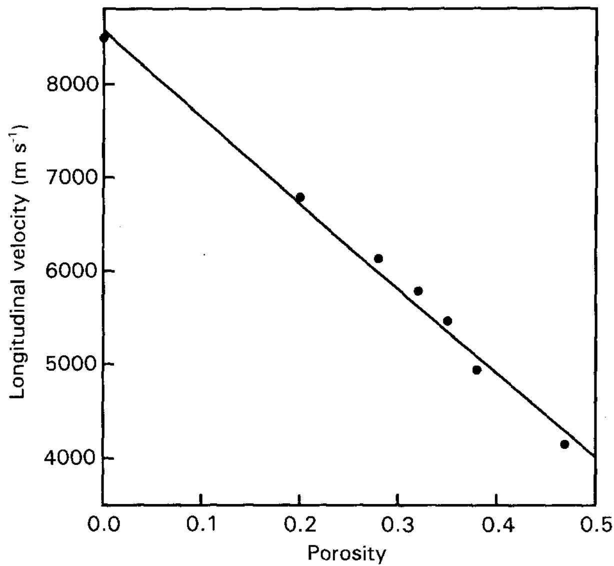

Figure 4 The plot of longitudinal velocity of the PS layer against porosity: (●) experimental values, (——) theoretical fit.

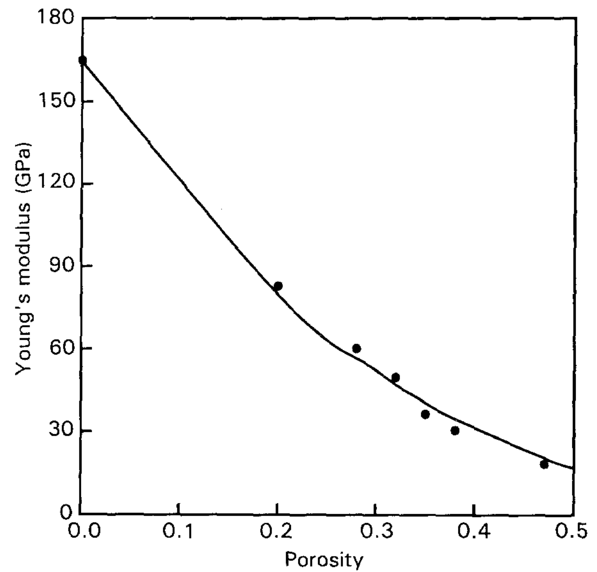

Figure 5 The Young's modulus of PS layers as a function of porosity: (●) measured values, (——) the theoretical fit.

shear velocities for non-porous silicon given elsewhere [9, 11]) and, in such a case, we can consider the constant B_0 as being the Young's modulus at zero porosity, E_0. Moreover, the value of velocity ratio between shear and longitudinal waves for non-porous silicon, X, is consistent with those found by other authors [21–24]. A plot of E against P for values of Young's modulus of porous silicon calculated from longitudinal, shear and Rayleigh velocities, and for the final result of the fit obtained by Equation 8, is shown in Fig. 5.

Equations 6–8 satisfy clearly the boundary conditions $V_L = V_{L0}$, $V_S = V_{S0}$ and $E = E_0$ for $P = 0$, and $V_L = 0$, $V_S = 0$ and $E = 0$ for $P = 1$. Phani *et al.* [25] showed that this kind of data fitting holds true over a wide range of porosity and does not have the limitations of linear and exponential empirical equations. Nevertheless, the equation for Young's modulus of porous materials suggested in this work differs from that proposed by those authors. This is due to the fact that shearing effects are not generally taken into account ($A = 1$ in Equation 4) when a specimen is submitted to tensile testing, which is justified because it has a very small shear dimension in comparison with its longitudinal dimension. However, the shearing effects, which are due to the shear polarization of acoustic waves, cannot be neglected when acoustic techniques are employed to characterize the elastic properties of solid materials, even if microscopic volumes are investigated. Equations 4 and 8 consider these effects and, therefore, they are different from those reported elsewhere [25].

The parameters k, m and s were also investigated by Phani *et al.* [25]. They observed that these quantities depend on the microstructure of the porous material and that the value of s lies between 2 and 4 ($0.5 < k$, $m < 1.5$) for a relatively ordered and less-open pore structure and higher for disordered and interconnected pore structure. Consequently, the values obtained for the parameters k and s indicate that the PS layers under consideration have a porous microstructure that can be considered nearly regular. Recent studies by transmission electron microscopy [6, 26–28] have confirmed this observation for porous silicon microstructure when the anodization conditions are well controlled. From Equation 11 we can say that q is also a microstructure-dependent parameter because it results from m and k. This parameter is obviously a measure of the influence of the pores upon the velocities of longitudinal and shear acoustic waves. For a given value of porosity, if $q > 0$, the shear velocity is more reduced than the longitudinal velocity and, inversely if $q < 0$. When q tends to zero the pores have the same influence upon the two bulk acoustic waves and the parameter A is independent of porosity. Although the plot of V_s against P is not shown, the values of V_{S0} and m were found to be 5840 m s^{-1} and 1.19, respectively. Substituting the values of k and m in Equation 11, we find $q = 0.19$. This value is nearly equal to that obtained from the Young's modulus data fitting. Likewise, we must note that the value of s, 3.22, is close to the expected value of $s = 3.19$ (see Equation 12). These last results confirm that the experimental errors were reduced in our acoustic study of PS layers. In a future work about PS layers, acoustic techniques will be employed to investigate the effect of different anodization conditions and pore morphology on these empirical parameters.

4. Conclusions

We have shown that acoustic techniques, more specifically acoustic microscopy and microechography, are very powerful non-destructive methods to characterize porous silicon layers, unlike conventional mechanical tests. Besides thickness measurements, the first attempts at using these techniques give valuable information about the porosity dependence of longitudinal and shear velocities and Young's modulus. Empirical equations obeying the boundary conditions have been proposed to relate the elastic properties to porosity. The values of the empirical constants k, m, s

and q were determined and they indicated that the porous silicon microstructure is relatively ordered. As mentioned in the text, additional experimental work will be carried out in order to investigate the influence of the anodization conditions and pore morphology upon the empirical constants and, consequently, elastic properties. Moreover, PS layers with high porosity will be also characterized by acoustic techniques. In future, this will enable a complete control of the mechanical parameters of PS layers during manufacturing.

Acknowledgements

R. J. M. da Fonseca acknowledges CNPq (Brazilian Council for Scientific and Technological Development) for personal financial support. This work was carried out under "l'accord programme Franco-Algérien no. 90 MDU 152".

References

1. D. R. TURNER, *J. Electrochem. Soc.* **105** (1958) 402.
2. L. T. CANHAM, *Appl. Phys. Lett.* **57** (1990) 1046.
3. K. IMAI, *Solid-State Electron.* **24** (1981) 159.
4. R. HERINO, G. BOMCHIL, K. BARLA, C. BERTRAND and J. L. GINOUX, *J. Electrochem. Soc. Solid-State Sci. Technol.* **134** (1987) 1994.
5. M. GRONAUER and J. FRICKE, *Acustica* **59** (1986) 177.
6. M. D. DRORY, P. C. SEARSON and L. LIU, *J. Mater. Sci. Lett.* **10** (1991) 81.
7. C. F. QUATE, *IEEE Trans.* **SU-32** (1985) 132.
8. J. ATTAL, A. SAIED, J. M. SAUREL and C. C. LY, in "Proceedings of the 17th International Symposium on Acoustic Imaging", June 1988, edited by H. Shimizu, N. Chubachi and J. Kushibiki (Plenum, New York, 1989) p. 121.
9. A. BRIGGS, "Acoustic Microscopy", (Clarendon, Oxford, 1992).
10. R. J. M. DA FONSECA, L. FEDJ-ALLAH, G. DESPAUX, A. BOUDOUR, L. ROBERT and J. ATTAL, *Adv. Mater.* **5** (1993) 508.
11. E. DIEULESAINT and D. ROYER, "Ondes Elastiques dans le Solides" (Masson, Paris, 1974) p. 155.
12. J. ATTAL, B. BIANCO, A. CAMBIASO, D. E. CREES, P. DARGENT, F. FASCE, D. R. NEWCOMBE, J. C. NOACK, J. M. SAUREL and M. ZAMBELLI, in "Proceedings of the 19th International Symposium on Acoustic Imaging", June 1991, edited by H. Ermert and H.-P. Hayer (Plenum, New York, 1992) p. 723.
13. I. A. VIKTOROV, "Rayleigh and Lamb Waves: Theory and Applications" (Plenum, New York, 1967) p. 26.
14. J. GOMEZ MORALES, R. RODRIGUEZ, J. DURAND, H. FERDJ-ALLAH, Z. HADJOUB, J. ATTAL and A. DOGHMANE, *J. Mater. Res.* **6** (1991) 2484.
15. A. VARY and R. F. LARK, *J. Test. Eval.* **7** (1979) 185.
16. A. VARY and K. J. BOWELS, *Polym. Eng. Sci.* **19** (1979) 373.
17. J. GROSS, G. REICHENAUER and J. FRICKE, *J. Phys. D Appl. Phys.* **21** (1988) 1447.
18. C. M. SAYERS and R. L. SMITH, *Ultrasonics* **20** (1982) 201.
19. D. G. ALBERT, *J. Appl. Phys.* **73** (1993) 28.
20. J. A. CAMPBELL, M. MATHISON, P. POOK and A. WYATT, "Up and Running with ASYST 2.0" (ASYST, Rochester, 1992).
21. E. M. CONWELL, *Proc. IRE* **50** (1952) 1327.
22. B. A. AULD, "Acoustic Fields and Waves in Solids", Vol. 1, (Wiley, New York, 1973) p. 371.
23. R. W. KEYES, *IEEE Trans.* **SU-29** (1982) 99.
24. P. J. BURNETT and G. A. D. BRIGGS, *J. Mater. Sci.* **21** (1986) 1828.
25. K. K. PHANI, S. K. NIYOGI, A. K. MAITRA and M. ROYCHAUDHURY, *ibid.* **21** (1986) 4335.
26. J. HARSANYI and H. U. HABERMEIER, *Microelectron. Eng.* **6** (1987) 575.
27. S.-F. CHUANG, S. D. COLLINS and R. L. SMITH, *Appl. Phys. Lett.* **55** (1989) 1540.
28. O. TESCHKE, M. C. GONÇALVES and F. GALEMBECK, *ibid.* **63** (1993) 1348.

Received 7 March
and accepted 9 June 1994